J Biol Inorg Chem (2007) 12:691–698
DOI 10.1007/s00775-007-0219-9

ORIGINAL PAPER

Mediated catalysis of *Paracoccus pantotrophus* cytochrome *c* peroxidase by *P. pantotrophus* pseudoazurin: kinetics of intermolecular electron transfer

P. M. Paes de Sousa · S. R. Pauleta · M. L. Simões Gonçalves · G. W. Pettigrew · I. Moura · M. M. Correia dos Santos · J. J. G. Moura

Received: 26 October 2006 / Accepted: 31 January 2007 / Published online: 15 March 2007

Abstract This work reports the direct electrochemistry of *Paracoccus pantotrophus* pseudoazurin and the mediated catalysis of cytochrome *c* peroxidase from the same organism. The voltammetric behaviour was examined at a gold membrane electrode, and the studies were performed in the presence of calcium to enable the peroxidase activation. A formal reduction potential, $E^{0\prime}$, of 230 ± 5 mV was determined for pseudoazurin at pH 7.0. Its voltammetric signal presented a pH dependence, defined by p*K* values of 6.5 and 10.5 in the oxidised state and 7.2 in the reduced state, and was constant up to 1 M NaCl. This small copper protein was shown to be competent as an electron donor to cytochrome *c* peroxidase and the kinetics of intermolecular electron transfer was analysed. A second-order rate constant of $1.4 \pm 0.2 \times 10^5$ M^{-1} s^{-1} was determined at 0 M NaCl. This parameter has a maximum at 0.3 M NaCl and is pH-independent between pH 5 and 9.

P. M. Paes de Sousa · S. R. Pauleta · I. Moura · J. J. G. Moura
ReQuimte, Centro de Química Fina e Biotecnologia,
Departamento de Química,
Faculdade de Ciências e Tecnologia,
Universidade Nova de Lisboa,
2829-516 Caparica, Portugal

M. L. Simões Gonçalves · M. M. Correia dos Santos (✉)
Centro de Química Estrutural,
Instituto Superior Técnico,
Av. Rovisco Pais,
1049-001 Lisboa, Portugal
e-mail: mcsantos@ist.utl.pt

G. W. Pettigrew
Royal (Dick) School of Veterinary Studies,
University of Edinburgh,
Summerhall, Edinburgh EH9 1QH, UK

Keywords Pseudoazurin · Cytochrome *c* peroxidase · Catalysis · Voltammetry · Intermolecular electron transfer

Abbreviations

CCP	Cytochrome *c* peroxidase
PAz	Pseudoazurin
SHE	Standard hydrogen electrode

Introduction

The incomplete reduction of molecular oxygen to water results in the formation of hydrogen peroxide, a species that can induce cell damage or death owing to its ability to form free radicals. Hydrogen peroxide can be removed by catalases in a dismutation reaction or reduced to water by peroxidases [1].

Periplasmic cytochrome *c* peroxidase (CCP) from *Paracoccus pantotrophus* is a calcium-containing dimeric enzyme of 37.5-kDa dihaemic subunits that catalyses the two-electron reduction of H_2O_2 to H_2O with oxidation of the physiological electron donor [2, 3]. This enzyme is isolated in a fully oxidised state (inactive), in which one haem (centre I), the high-potential haem, is in a high-spin/low-spin equilibrium and the other haem (centre II), the low-potential haem, is low-spin. During the catalytic mechanism, centre I acts as an electron-transfer centre, accepting incoming electrons and transferring them to the peroxidatic haem (centre II). The entry of one electron to the high-potential haem leads to a complex change of spin states and redox potential of both haems. The mechanism involves strong haem–haem interactions and structural changes that are more dramatic around the peroxidatic

haem, in order to attain a mixed-valence ''ready state'' for binding, reduction and cleavage of peroxide [4, 5].

The conformational transitions induced by the redox state change of centre I and associated with the formation of the active peroxidatic haem are dependent on the presence of bound calcium [6–9]. This activation reaction results in the transition of the low-potential haem to a high-spin state with the loss of one histidine ligand, allowing substrate binding. The redox transitions of the two haems have been studied using different techniques, such as visible spectroscopy, electron paramagnetic resonance and NMR [6–10].

The crystal structure of *P. pantotrophus* CCP was obtained in two different redox states, a fully oxidised form and a mixed-valence form, which supports these observations [11]. The comparison of these two structures revealed that the inactive form presents a closed conformation where the peroxidatic haem adopts a hexacoordinate structure, hindering the peroxidatic reaction from taking place. The active mixed-valence form shows conformational changes in four different loop regions and the peroxidatic haem becomes pentacoordinate, providing access of the substrate to the active site [11, 12].

Although *c*-type cytochromes and blue copper proteins are structurally very different, Williams et al. [13] proposed that they share features of an electron-transfer surface that confers ''pseudospecificity'' in their interactions with a range of redox partners. Pseudoazurin (PAz) is proposed to be one of the electron carriers in the periplasm of the bacteria, shuttling electrons between the cytochrome bc_1 complex and several periplasmic enzymes involved in denitrification as well as CCP [14, 15]. Another small redox protein, cytochrome c_{550}, has also been identified as the electron donor to these enzymes [14, 15].

P. pantotrophus PAz is a small copper protein of 13.4 kDa which has a net charge of –4 at pH 7.0 and a very large dipole moment. The positive dipole vector is positioned at the proposed electron-transfer site, His81, and is thought to be instrumental in the preorientation of the molecule for electron transfer. In previous kinetics studies, PAz was shown to be competent as an alternative electron donor to *P. pantotrophus* CCP and to bind at the same site on the CCP surface as cytochrome c_{550} [16, 17].

Direct electrochemistry of redox proteins and enzymes attracts widespread interest since the protein–electrode surface recognition process can provide a model for the electron transfer in biological systems. Information regarding the thermodynamics, kinetics and mechanisms of the biological electron transfers and reactions coupled to electron transfer is accessible with electrochemical techniques [18]. A wide range of working electrodes and strategies can be used in order to characterise and understand the physiological functions of redox proteins and enzymes [19, 20].

Several works have reported the direct electrochemistry of blue copper proteins, including PAz from *Achromobacter cycloclastes* [21, 22] and from *Alcaligenes faecalis* [23]. Few works dealing with the electrochemistry of other peroxidases have been published, with monohaem CCP being the most studied [24, 25]. The first reports on bacterial CCPs, from *P. pantotrophus* and from *Nitrosomonas europaea*, were recently published [26, 27].

This work reports the first electrochemical study of the electron transfer between CCP and one of its physiological electron donors, PAz. The direct electron transfer to PAz and the mediated electrochemical behaviour of CCP were analysed by cyclic voltammetry at a gold electrode using the membrane electrode configuration [28]. This configuration has several important advantages, in particular the use of very small volumes of protein (approximately 2 µl), the ease of electrode preparation and low cost, as well as the capacity to rapidly investigate experimental parameters with the same protein sample. The pH dependence of *P. pantotrophus* PAz formal reduction potential was analysed and three p*K* values were identified. The intermolecular electron-transfer rate constant between these two proteins was determined and the effects of pH and ionic strength on this parameter were analysed.

Materials and methods

Protein isolation and purification

P. pantotrophus PAz and CCP were isolated and purified as described before [2, 16]. The concentration of the proteins was determined spectrophotometrically using the extinction coefficient at 590 nm, $\varepsilon = 3.00\ \mathrm{mM^{-1}\ cm^{-1}}$, and 409 nm, $\varepsilon = 250\ \mathrm{mM^{-1}\ cm^{-1}}$, for the oxidised PAz and fully oxidised CCP, respectively [2, 16].

Procedures

The compounds neomycine, 4,4′-dithiodipyridine and $CaCl_2$ were obtained from Sigma and all other chemicals were pro analysis grade. All solutions used in the studies were prepared with Milli-Q water.

Voltammetric measurements were performed using a potentiostat/galvanostat AUTOLAB PSTAT10 from ECO Chemie (Utrecht, The Netherlands), as the source of applied potential and as a measuring device. The whole system was controlled and the data were analysed with the GPES software package from ECO Chemie. The scan rate varied between 5 and 200 mV s^{-1}. Throughout the paper,

all potential values are referred to the standard hydrogen electrode (SHE).

A conventional three-electrode configuration cell was used, with a platinum auxiliary electrode and an Ag/AgCl reference electrode (BAS MF-2052; 205 mV vs. SHE). The working electrode was a gold disk electrode from BAS (MF-2014) with a nominal radius of 0.8 mm. The effective surface area of the electrode was determined from its response in a known concentration of the ferrocyanide/ferricyanide couple ($D = 7.84 \times 10^{-6}$ cm^2 s^{-1} [29]) and was found to be 0.0195 cm^2.

Electrode preparation

Before each experiment, the gold disk electrode was polished by hand on a polishing cloth (Buehler 40-7212) using a water–alumina (0.05 μm) slurry (Buehler 40-6365-006), sonicated for 5 min, rinsed well with Milli-Q water and finally dipped into 1 mM 4,4′-dithiodipyridine solution for 5 min. The membrane configuration was prepared as previously described [28] using a negatively charged Spectra/Por MWCO 3500 membrane.

Electrolyte

In typical experiments, the supporting electrolyte, as well as the working solution, contained 10 or 50 mM phosphate buffer pH 7.0 ± 0.1, 0.5 mM 4,4′-dithiodipyridine and, whenever CCP was present, 1 mM $CaCl_2$ to enable the enzyme activation. PAz was present in a concentration of 218 μM and CCP varied between 1.04 and 23.1 μM.

In the experiments with a saturating concentration of substrate, 1 mM H_2O_2 was present in the electrolyte solution. Studies with substrate concentration were done by varying H_2O_2 between 20 μM and 3 mM.

The pH of the electrolyte was varied from 5 to 11 by adding small amounts of 5 M HCl or 2 M NaOH to 10 mM acetate, 2-morpholinoethanesulfonic acid, phosphate, tris(hydroxymethyl)aminomethane–HCl or *N*-cyclohexyl-3-aminopropanesulfonic acid buffer solutions. As to the ionic strength, the variation was carried out by adding increasing amounts of NaCl (up to 1 M).

All solutions were deaerated for 30 min with u-type nitrogen, and all measurements were performed at least in duplicate in a temperature-controlled room at 20 ± 1 °C.

Results and discussion

Direct electrochemistry of *P. pantotrophus* PAz

Typical cyclic voltammograms of PAz at the gold membrane electrode in the presence of 4,4′-dithiodipyridine can be observed in Fig. 1. Similar voltammograms were obtained in the absence of promoter, although the response was less stable during repeated potential cycling.

From the analysis of the cyclic voltammograms in terms of potentials and peaks currents, PAz was a reversible system with two different behaviours in the scan rate (v) range, as can be observed in Fig. 2: control by diffusion, with the peak currents (i_p) varying linearly with $v^{1/2}$ (Fig. 2a), for the highest scan rates ($100 \leq v \leq 200$ mV s^{-1}); and thin-layer behaviour, with i_p varying linearly with v (Fig. 2b), for the lowest scan rates ($v < 100$ mV s^{-1}).

The ratio of the cathodic (i_{pc}) and anodic (i_{pa}) peak currents was close to 1 for all scan rates. In the whole range of v, peak-to-peak separation, $E_{pa} - E_{pc}$, remained constant at 12 mV. The width at half height ($\Delta E_{p,1/2}$) was also constant for the cathodic and anodic peaks and close to 90 mV. The behaviour described corresponds to a reversible one-electron process ($Cu^{2+} + e^- \leftrightarrow Cu^+$) in terms of thin-layer theory [28, 30, 31], so in this situation the formal reduction potential can be estimated from the average of the reduction and oxidation peak potentials and a value of $E^{0\prime} = (E_{pc} + E_{pa})/2 = 230 \pm 5$ mV was obtained, for pH 7.0. This value compares well with the formal potential (230 mV, same pH) estimated by cyclic voltammetry in [14].

The effect of pH on the formal reduction potential of PAz was analysed in the range 5–11. This is easily done at a membrane electrode since, while the protein molecules stay entrapped in close vicinity to the electrode surface, small ions diffuse through the membrane [28]. The absence of a PAz electrochemical signal below pH 5 and above pH 11 established those limits.

As shown in Fig. 3, PAz has a pH dependence of the redox potential defined by two equilibria and three pK values. The data can be fitted to Eq. 1, according to the

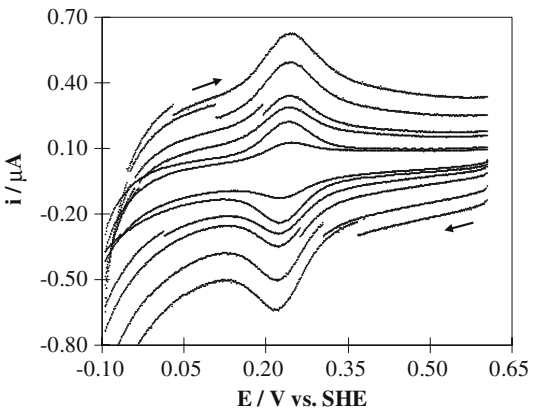

Fig. 1 Cyclic voltammograms ($35 < v < 200$ mV s^{-1}) at the gold membrane electrode (AUME) of 218 μM pseudoazurin (PAz) in 50 mM phosphate buffer, pH 7.0 and 0.5 mM 4,4′-dithiodipyridine

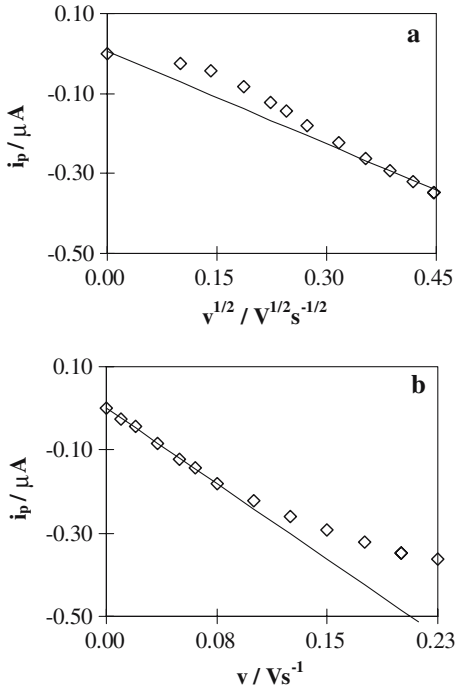

Fig. 2 Variation of the peak current (from the cyclic voltammograms in Fig. 1) with the square root of the scan rate (**a**) and the scan rate (**b**)

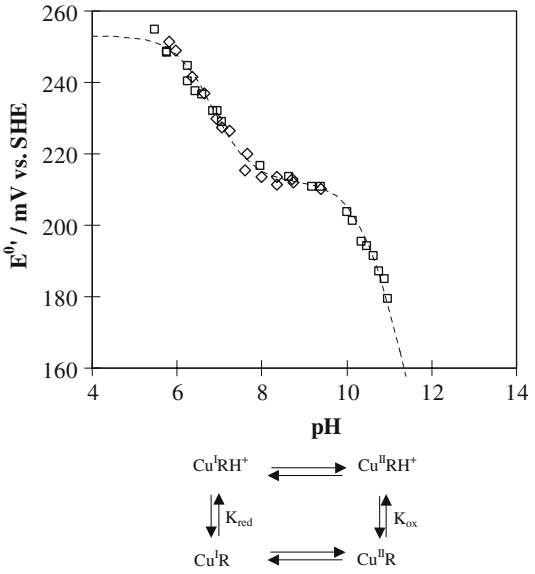

Fig. 3 Effect of pH on PAz formal reduction potential, $E^{0\prime}$. *Diamonds* and *squares* two different experiments; *line* fitting to Eq. 1. Cyclic voltammograms (v = 50 mV s^{-1}) at the AUME of 218 μM PAz in different buffer systems and 0.5 mM 4,4′-dithiodipyridine. *Scheme*: Proton dissociation equilibria for one pK pair

hypothetical set of equilibria shown in the inset of Fig. 3 [32]:

$$E^{0\prime} = E^{0\prime}_{lp} - \frac{RT}{nF}\left(\frac{[H^+]^2 + K_{O1}[H^+] + K_{O1}K_{O2}}{[H^+]^2 + K_R[H^+]}\right), \qquad (1)$$

where $E^{0\prime}$ is the measured reduction potential, $E^{0}_{lp}{}'$ is the reduction potential at low pH, and K_O and K_R are the proton dissociation constants of the oxidised and reduced forms, respectively. A nonlinear regression fit (with no fixed parameters), using the CERN library Fortran program MINUIT algorithm, gave the values $E^{0}_{lp}{}' = 253 \pm 3$ mV, p$K_{O1} = 6.5 \pm 0.2$, p$K_R = 7.2 \pm 0.1$ and p$K_{O2} = 10.5 \pm 0.1$.

Some of the pK values can be assigned from spectroscopic evidence for this PAz [16], by comparison with the results obtained for PAz from *Achromobacter cycloclastes* [22, 33, 34], which has 67% homology with *P. pantotrophus* PAz. The pK values of 6.5 and 7.2 have been assigned to the protonation of the histidine residue 6 [33]. The pK_{O2} value of 10.5 may be attributed, but this is still in discussion, to a structural transition brought about by the acid dissociation of the NH_3^+ ε-amino group of Lys77 (pK_a = 10.4) [22].

The ionic strength dependence of the formal reduction potential was also studied. Increasing amounts of NaCl were added to the electrolyte solution and the PAz signal was shown to be independent of ionic strength, in the range 0–1 M (data not shown). This result suggests that the interaction with the electrode is mainly governed by forces like hydrophobic or hydrogen-bonding interactions rather than electrostatic interactions. A favourable domain for electron transfer to occur must be due to a suitable hydrogen-bonding interaction between the pyridyl nitrogen atoms of the promoter and the residues on the protein surface. It is interesting to note that the negative charge of the membrane seems not to affect the redox reaction of the negatively charged PAz.

Catalytic activity of *P. pantotrophus* CCP with *P. pantotrophus* PAz as an electron donor

The catalytic activity of *P. pantotrophus* CCP towards *P. pantotrophus* PAz was then investigated at the gold membrane electrode (Fig. 4). Working solutions of 218 μM PAz and different CCP concentrations were prepared, and 0.5 mM 4,4′-dithiodipyridine and 1 mM Ca^{2+} (for the enzyme activation) were present both in the working solutions and in the electrolyte.

Similar voltammograms to those obtained for PAz alone were observed for PAz in the presence of CCP (Fig. 4, voltammogram a). However, it is clear in the same figure that a sigmoidal waveform develops when a saturating concentration of H_2O_2 (1 mM) is added to the electrolyte (voltammograms b–e). Moreover, voltammograms from solutions containing only CCP either in the presence or in the absence of H_2O_2 were indistinguishable from the background current (data not shown).

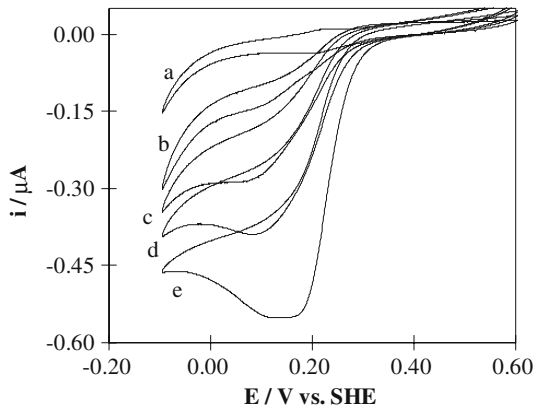

Fig. 4 Cyclic voltammograms (v = 5 mV s^{-1}) at the AUME of 218 μM PAz and increasing concentrations of cytochrome *c* peroxidase (CCP): *a*, *b* 1.04 μM, *c* 4.62 μM, *d* 10.4 μM and *e* 23.1 μM; 1 mM H_2O_2 in all cases, except *a*, where it was absent from the electrolyte. Medium, 10 mM phosphate buffer pH 7.0, 0.5 mM 4,4′-dithiodipyridine and 1 mM $CaCl_2$

The half-wave potential of the sigmoidal waves ($E_{1/2}$ = 218 ± 14 mV ≡ $E^{0\prime}$ [35]) shows that the actual transfer process is the catalysed reduction of PAz. The catalytic current obtained is independent of the scan rate up to 100 mV s^{-1} and increases for increasing CCP concentration. This behaviour is consistent with a reaction mechanism involving an initial heterogeneous electron-transfer reaction at the electrode (Fig. 5, step 1), followed by homogeneous chemical reactions: the oxidised form of PAz is regenerated by CCP (Fig. 5, step 2) which, in turn, is recycled by hydrogen peroxide (Fig. 5, step 3). This mechanism can be simplified to

$$\begin{aligned} &\mathrm{PAz_{ox}} + e^- \leftrightarrow \mathrm{PAz_{red}} \\ &\mathrm{PAz_{red}} + \mathrm{CCP} \rightarrow \mathrm{PAz_{ox}} \end{aligned} \tag{2}$$

provided that the following conditions are obeyed: (1) the heterogeneous electron transfer (Fig. 5, step 1) is a reversible reaction; (2) the homogeneous chemical reaction (Fig. 5, step 2) is irreversible; (3) the reaction between PAz and CCP is pseudo first order with a reaction rate constant given by $k' = kC_{CCP}$, where k is the second-order rate constant and C is the concentration.

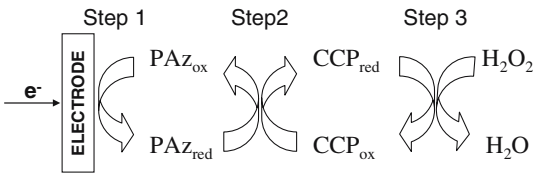

Fig. 5 Mediation scheme for CCP: the electrode reduces PAz, which is immediately reoxidised by CCP; the level of oxidised CCP is then restored by conversion of hydrogen peroxide to water

The first condition is well obeyed as previously demonstrated. Owing to the excess of hydrogen peroxide in solution, CCP is reoxidised in the catalytic cycle (Fig. 5, step 3), and not by transferring electrons back to PAz. Therefore, step 2 (Fig. 5) can be considered irreversible and condition 2 is fulfilled. As to condition 3, it implies that CCP is present in large excess. The enzyme is not present in excess over PAz but, owing to the saturating concentration of hydrogen peroxide, this requisite is obeyed if the rate of recycling of oxidised CCP by H_2O_2 is not rate-limiting. In this case, CCP will always be available to react with PAz and pseudo-first-order conditions are met.

The theory describing such a mechanism for diffusion-controlled processes was developed by Nicholson and Shain [36] and applied to several kinetics studies of reactions between mediators and redox proteins [37] (and references therein). However, since the catalytic current observed in our experimental conditions is independent of the scan rate for v < 100 mV s^{-1}, thin-layer theory must be considered following Laviron's treatment for diffusionless electrochemical systems [31]. Cyclic voltammetry curves were recorded in the scan rate range 5–100 mV s^{-1} for 218 μM PAz and increasing CCP concentrations, in the absence and presence of an excess of H_2O_2. From these recordings, the peak current (i_p) and the catalytic peak current (i_{cat}) were measured. The peak current is given by

$$i_p = \frac{n^2F^2vVC_{PAz}}{4RT} \tag{3}$$

whereas the catalytic current is given by

$$i_{cat} = nFk'VC_{PAz} \tag{4}$$

In these equations, V is the entrapped solution volume, C is the concentration and the other terms have their usual meaning. The pseudo-first-order rate constant for the intermolecular electron-transfer reaction, k', can be determined from the slope of the (i_{cat}/i_p) versus ($1/v$) plot:

$$\left(i_{cat}/i_p\right) = (4RT/nF)k'(1/v). \tag{5}$$

From the plot of k' for different CCP concentrations (C_{CCP}), the second-order rate constant, k, is then estimated.

In Fig. 6a, a plot of (i_{cat}/i_p) versus ($1/v$) for different CCP concentrations is presented. A linear dependence is verified, between 4.5 and 20 μM CCP, demonstrating that all requirements of the model are met. This implies that the intermolecular electron transfer between PAz and CCP limits the overall reaction rate. An intermolecular electron-transfer rate constant $k = (1.5 \pm 0.2) \times 10^5$ M^{-1} s^{-1} was estimated from the variation of k' with CCP concentration (Fig. 6b).

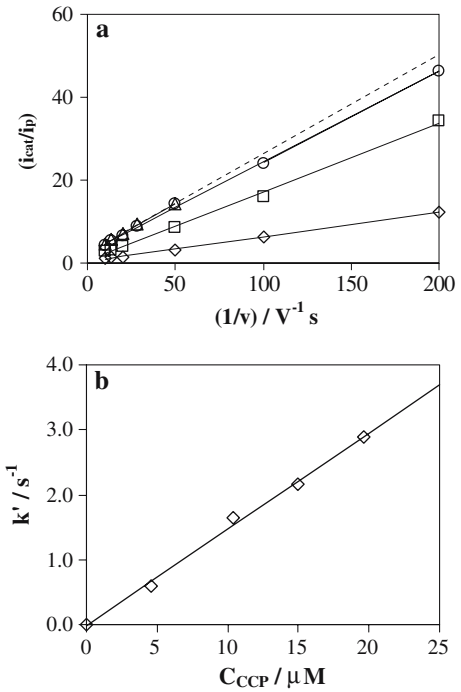

Fig. 6 **a** (i_{cat}/i_p) versus ($1/v$) for *diamonds* 4.62 μM, *squares* 10.4 μM, *circles* 15 μM and *triangles* 19.6 μM CCP. **b** The pseudo-first-order rate constant versus CCP concentration

The intermolecular rate constant can also be calculated with the methodology proposed first by Savéant and Vianello [38] and developed later by Coury et al. [39], from the value of the H_2O_2 saturated limiting current given by Eq. 4.

As to the entrapped solution volume, V, it can be computed using Eq. 3 from the dependence on the scan rate of either the cathodic or the anodic peak currents of the cyclic voltammograms for solutions containing both PAz and CCP in the absence of hydrogen peroxide. A volume of $(1.2 \pm 0.1) \times 10^{-5}$ cm^3 was estimated, in very good agreement with previous results at the same electrode [28]. Calculations using Eq. 4 gave $k = (1.2 \pm 0.3) \times 10^5$ M^{-1} s^{-1} in accordance with the value determined above.

The effect of pH and ionic strength on the intermolecular rate constant was then analysed and although k was shown to be pH-independent in the range 5–9 (data not shown), it varied with NaCl concentration (data not shown). In the ionic strength studies, a bell-shaped curve with a peak of activity at about 0.3 M NaCl was obtained, for which the intermolecular rate constant at high NaCl concentration (2.0×10^5 M^{-1} s^{-1}) was slightly higher than the value determined in the absence of NaCl. The decrease of activity with further increasing NaCl concentration is consistent with the known electrostatic character of the complex between CCP and PAz, which is due to the positive dipole vector on PAz and the negative surface of CCP near the electron-transferring haem [16, 17].

Similar behaviour was observed for the steady-state kinetics activity of this enzyme with PAz as an electron donor [16]. However, in those studies the maximum value occurred at lower NaCl concentrations (about 30 mM) and very low activity was registered above 0.5 M. This difference may be due to the use of a charged membrane in the electrochemical studies. Somehow, the membrane favours the formation of the encounter complex and makes it less dependent on the ionic strength, in spite of the electrostatic forces that govern the interaction.

It must be pointed out that the PAz signal showed no dependence on the ionic strength, which is consistent with the interaction established between PAz and the electrode interface not being electrostatic in nature, as mentioned already. Thus, PAz must interact with the electrode in such a way that the hydrophobic patch surrounded by the lysine's ring is free to interact with its redox partner.

As to the pH, no effect was observed in the range from 5 to 9, but no catalytic current develops above pH 9. As mentioned before, the lower limit is due to the loss of the PAz signal, and the absence of catalytic activity above pH 9 can be attributed to the inactivation of CCP, since the PAz signal is maintained between pH 9 and 11. The absence of a pK pair around 7, as observed for PAz alone, suggests that CCP has a pK pair around this same value.

Another set of experiments were performed by varying the hydrogen peroxide concentration in the electrolyte, for a constant PAz and CCP mixture. The results are presented in Fig. 7 and it is clear that the peak current of PAz increases with successive additions of hydrogen peroxide until the peaklike signal is converted to a sigmoidal wave form.

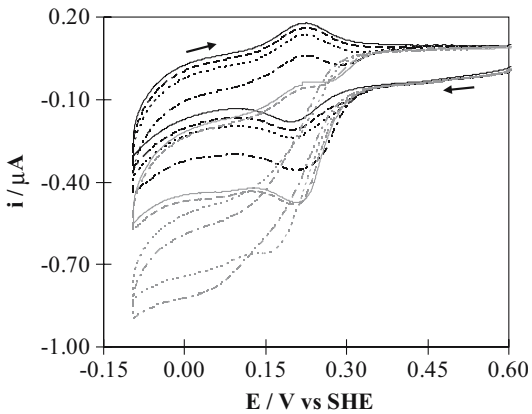

Fig. 7 Cyclic voltammograms (v = 50 mV s^{-1}) at the AUME of 218 μM PAz and 10.4 μM CCP in the presence of increasing concentrations of H_2O_2 (μM): 0 (*solid black line*), 20.0 (*dashed black line*), 49.8 (*dotted black line*), 99.4 (*dash-dotted black line*), 199 (*solid grey line*), 297 (*dashed grey line*), 495 (*dotted grey line*) and 741 (*dash-dotted grey line*). Medium, 10 mM phosphate buffer pH 7.0, 0.5 mM 4,4′-dithiodipyridine and 1 mM $CaCl_2$

The difference between the measured current, for each hydrogen peroxide addition and the current in the absence of hydrogen peroxide ($i_p - i_{p(0)} = i_{cat}$) was plotted versus substrate concentration (Fig. 8). This catalytic current increases until 1 mM hydrogen peroxide and decreases for higher concentrations.

Above 1 mM, hydrogen peroxide most probably destroys the enzyme and consequently a lower catalytic activity is observed. For concentrations up to 1 mM, the results were fitted to Michaelis–Menten kinetics, using the CERN library Fortran program MINUIT algorithm. Since thin-layer conditions were verified, the Michaelis–Menten equation has the form

$$i_{cat} = \frac{i_{max}\ C_{H_2O_2}}{C_{H_2O_2} + K_M} = \frac{nFk'VC_{PAz}C_{H_2O_2}}{C_{H_2O_2} + K_M} \quad (6)$$

where i_{max} is the catalytic current observed at the maximum rate and K_M is the Michaelis–Menten constant. As can be seen in Fig. 8, the fitting shows that the experimental data are in good agreement with Eq. 6, leading to a K_M of 390 μM and an intermolecular electron-transfer rate constant, k, of $(1.6 \pm 0.2) \times 10^5$ M^{-1} s^{-1}. This result again confirms that PAz is an electron donor to CCP.

The good agreement among all k values means that all requirements of the model (Fig. 5) are met. The overall reaction is neither limited by the CCP reduction of H_2O_2 (step 3, which includes an intramolecular electron transfer between the two CCP haems) nor by the PAz reduction at the electrode (step 1). Therefore, the intramolecular rate constant k_{intra} must be similar to or higher than $k \times C_{PAz}$. Taking an average value for the intermolecular rate constant between PAz and CCP, $1.4 \pm 0.2 \times 10^5$ M^{-1} s^{-1}, pH 7, 0 M NaCl, we can estimate a minimum value for the intramolecular rate constant of 30 s^{-1}.

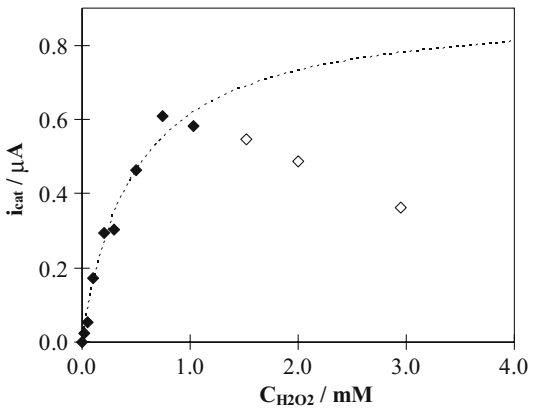

Fig. 8 Variation of the catalytic current with H_2O_2 concentration (same conditions as in Fig. 7). The *closed diamonds* were fitted to Michaelis–Menten kinetics (Eq. 6), using the CERN library Fortran program MINUIT algorithm

Conclusions

In the present work, cyclic voltammetry and a gold membrane electrode were used for the first time to analyse the direct electron transfer to *P. pantotrophus* PAz and to probe its interaction with one of its physiological partners, CCP.

PAz isolated from *P. pantotrophus* has a formal reduction potential of 230 ± 5 mV, at pH 7.0, and three p*K* values were identified, 6.5, 7.2 and 10.5, from the dependence of that parameter with the pH, as verified for other small blue copper proteins [22, 33, 34].

In this work *P. pantotrophus* PAz was shown to be an active electron donor to *P. pantotrophus* CCP with a second-order rate constant, $1.4 \pm 0.2 \times 10^5$ M^{-1} s^{-1}. This value compares well with other intermolecular rate constants determined using cyclic voltammetry. Two examples are the electron transfer from *Achromobacter cycloclastes* PAz to its electron donor, nitrite reductase, that was determined to have a k value of 7.3×10^5 M^{-1} s^{-1} [40], and the complex between cytochrome c_{552} and cytochrome cd_1 nitrite reductase isolated from *Pseudomonas nautica*, with a k value of 2.8×10^5 M^{-1} s^{-1} [37].

The kinetics of intermolecular electron transfer was pH-independent, between pH 5 and 9. It would seem unlikely that the absence of a p*K* pair around 7, as observed for PAz alone, occurs by chance. This suggests that the two redox partners have evolved to match their p*K* values to ensure a constant ΔE_m driving force for electron transfer to occur over varying pH.

The rate constant had a maximum value at 0.3 M NaCl and decreased at higher NaCl concentration, as expected for an interaction governed by electrostatic forces. The use of a charged membrane, however, seems to favour the formation of the encounter complex and makes it less dependent on ionic strength, in comparison with the results obtained by steady-state kinetics [16]. The results obtained also indicate that PAz interacts with the electrode through hydrophobic forces, which do not affect the formation of the encounter complex with the enzyme.

It is also important to point out that the membrane configuration is an interesting strategy for the cases in which adsorption of a protein to the electrode surface is not successfully achieved, hindering the use of protein film voltammetry [18]. This configuration also enables the use of very small protein volumes (2 μl). The entrapment of the proteins between the membrane and the electrode surface enables the achievement of thin-layer conditions, and avoids the problems concerning diffusion.

Acknowledgements We would like to thank Andreia Mestre for some experimental assistance. This work is within the research project POCI/QUI/55743/2004. P.M.P.S. and S.R.P. thank Fundação para

a Ciência e Tecnologia for financial support (SFRH/BPD/14099/2003 and SFRH/BPD/14067/2003, respectively).

References

1. Halliwell B, Gutteridge JMC (eds) (1989) Free radicals in biology and medicine. Oxford Science, Oxford
2. Goodhew CF, Wilson IBH, Hunter DJB, Pettigrew GW (1990) Biochem J 271:707–712
3. Pettigrew GW (1991) Biochim Biophys Acta 1058:25–27
4. Gilmour R, Goodhew CF, Pettigrew GW, Prazeres S, Moura I, Moura JJG (1993) Biochem J 294:745–752
5. Gilmour R, Goodhew CF, Pettigrew GW, Prazeres S, Moura I, Moura JJG (1994) Biochem J 300:907–914
6. Prazeres S, Moura I, Moura JJG, Gilmour R, Goodhew CF, Pettigrew GW (1993) Magn Reson Chem 31:S68–S72
7. Prazeres S, Moura JJG, Moura I, Gilmour R, Goodhew CF, Pettigrew GW, Ravi N, Huynh BH (1995) J Biol Chem 270:24264–24269
8. Prazeres S, Moura I, Gilmour R, Pettigrew GW, Ravi N, Huynh BH (1995) In: La Mar G (eds) Nuclear magnetic resonance of paramagnetic molecules. Kluwer, Dordrecht, pp 141–163
9. Gilmour R, Prazeres S, McGinnity DF, Goodhew CF, Moura JJG, Moura I, Pettigrew GW (1995) Eur J Biochem 234:878–886
10. Gilmour R, Goodhew CF, Pettigrew GW, Prazeres S, Moura I, Moura JJG (1993) Biochem J 294:745–752
11. Echalier A, Goodhew CF, Pettigrew GW, Fulop V (2006) Structure 14:107–117
12. Pettigrew GW, Echalier A, Pauleta SR (2006) J Inorg Biochem 100:551–567
13. Williams PA, Fulop V, Leung YC, Chan C, Moir JW, Howlett G, Ferguson SJ, Radford SE, Hajdu J (1995) Nat Struct Biol 2:975–982
14. Berks BC, Baratta D, Richardson DJ, Ferguson SJ (1993) Eur J Biochem 212:467–476
15. Richter CD, Allen JWA, Higham CW, Koppenhöfer A, Zajicek RS, Watmough NJ, Ferguson SJ (2002) J Biol Chem 277:3093–3100
16. Pauleta SR, Guerlesquin F, Goodhew CF, Devreese B, Van Beeumen J, Pereira AS, Moura I, Pettigrew GW (2004) Biochem 43:11214–11225
17. Pauleta SR, Cooper A, Nutley M, Errington N, Harding S, Guerlesquin F, Goodhew CF, Moura I, Moura JJG, Pettigrew GW (2004) Biochem 43:14566–14576
18. Armstrong FA (2002) In: Bard AJ, Stratmann M, Wilson GS (eds) Encyclopedia of electrochemistry, vol 9. Bioelectrochemistry. Wiley, New York
19. Correia dos Santos MM, Paes de Sousa PM, Simões Gonçalves ML, Ascenso C, Moura I, Moura JJG (2001) J Electroanal Chem 501:173–179
20. Correia dos Santos MM, Paes de Sousa PM, Simões Gonçalves ML, Romão MJ, Moura I, Moura JJG (2004) Eur J Biochem 271:1329–1338
21. Sakurai T, Ikeda O, Suzuki S (1990) Inorg Chem 29:4715–4718
22. Kohzuma T, Dennison C, McFarlane W, Nakashima S, Kitagawa T, Inoue T, Kai Y, Nishio N, Shidara S, Suzuki S, Sykes AG (1995) J Biol Chem 270:25733–25738
23. Astier Y, Bond AM, Wijma HJ, Canters GW, Hill HA, Davis JJ (2004) Electroanalysis 16:1155–1165
24. Paddock RM, Bowden EF (1989) J Electroanal Chem 260:487–494
25. Mondal MS, Fuller HA, Armstrong FA (1996) J Am Chem Soc 118:263–264
26. Lopes H, Pettigrew GW, Moura I, Moura JJG (1998) J Biol Inorg Chem 3:632–642
27. Bradley AL, Chobot SE, Arcieros DM, Hoopers AB, Elliot SJ (2004) J Biol Chem 279:13297–13300
28. Correia dos Santos MM, Paes de Sousa PM, Simões Gonçalves ML, Krippahl L, Moura JJG, Lojou E, Bianco P (2003) J Electroanal Chem 541:153–162
29. Kakihana M, Ikeuchi H, Satô GP, Tokuda K (1980) J Electroanal Chem 108:381–383
30. Laviron E (1974) Electroanal Chem Interfacial Electrochem 52:355–393
31. Laviron E (1979) J Electroanal Chem 101:19–28
32. Moore GR, Pettigrew GW (eds) (1990) Cytochromes *c*: evolutionary, structural and physicochemical aspects. Springer, Berlin
33. Sato K, Dennison C (2002) Biochem 41:120–130
34. Dennison C, Kohzuma T (1999) Inorg Chem 38:1491–1497
35. Bard AJ, Faulkner LR (eds) (2001) Electrochemical methods, fundamentals and applications. Wiley, New York
36. Nicholson RS, Shain I (1964) Anal Chem 36:706–723
37. Lopes H, Besson S, Moura I, Moura JJG (2001) J Biol Inorg Chem 6:55–62
38. Savéant JM, Vianello E (1965) Electrochim Acta 10:905–920
39. Coury LA Jr, Oliver BN, Egekeze JO, Sosnoff CS, Brumfield JC, Buck RP, Murray RW (1990) Anal Chem 62:452–458
40. Kataoka K, Yamaguchi K, Kobayashi M, Mori T, Bokui N, Suzuki S (2004) J Biol Chem 279:53374–53378